Journal of Coordination Chemistry

ISSN: 0095-8972 (Print) 1029-0389 (Online) Journal homepage: http://www.tandfonline.com/loi/gcoo20

K(I)-M(II) (M = Co, Mn) heterometallic-(perfluorinated) organic frameworks containing inorganic layered K–O–M linkages: synthesis, crystal structure, and magnetic properties

Qi Yan, Xing-Cai Huang, Jing Zhong, Jian Gao, Sheng-Chun Chen, Ming-Yang He, Qun Chen & Michael A. Beckett

To cite this article: Qi Yan, Xing-Cai Huang, Jing Zhong, Jian Gao, Sheng-Chun Chen, Ming-Yang He, Qun Chen & Michael A. Beckett (2015) K(I)-M(II) (M = Co, Mn) heterometallic-(perfluorinated) organic frameworks containing inorganic layered K–O–M linkages: synthesis, crystal structure, and magnetic properties, Journal of Coordination Chemistry, 68:15, 2691-2702, DOI: 10.1080/00958972.2015.1057709

To link to this article: http://dx.doi.org/10.1080/00958972.2015.1057709

Published online: 30 Jun 2015.

Journal of Coordination Chemistry, 2015
Vol. 68, No. 15, 2691–2702, http://dx.doi.org/10.1080/00958972.2015.1057709

K(I)-M(II) (M = Co, Mn) heterometallic-(perfluorinated) organic frameworks containing inorganic layered K–O–M linkages: synthesis, crystal structure, and magnetic properties

QI YAN†§, XING-CAI HUANG†, JING ZHONG†, JIAN GAO‡, SHENG-CHUN CHEN*†‡, MING-YANG HE*†, QUN CHEN†‡ and MICHAEL A. BECKETT§

†Jiangsu Key Laboratory of Advanced Catalytic Materials and Technology, Changzhou University, Changzhou, PR China
‡School of Chemical Engineering, Nanjing University of Science & Technology, Nanjing, PR China
§School of Chemistry, Bangor University, Bangor, UK

(*Received 19 December 2014; accepted 9 April 2015*)

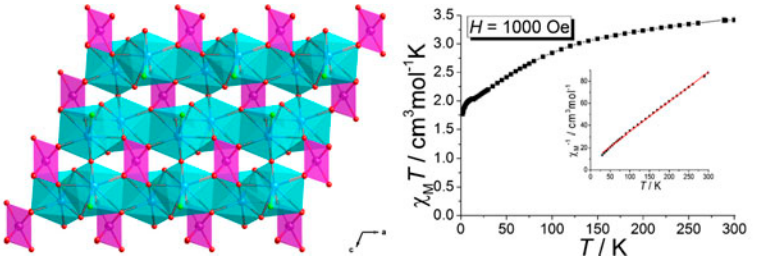

Reactions of a perfluorinated ligand, tetrafluorophthalic acid (o-H_2BDC-F_4), with KNO_3 and M $(OAc)_2$ (M = Co, Mn) led to the formation of perfluorinated metal-organic frameworks $[CoK_2(o\text{-BDC-}F_4)_2(MeOH)]_n$ (**1**) and $[MnK_2(o\text{-BDC-}F_4)_2(DMF)]_n$ (**2**). The structures were characterized by elemental analyses, infrared spectra, and single-crystal X-ray diffraction. Both complexes show similar 2-D heterometallic-organic frameworks containing unusual layered inorganic K–O–M connectivities. For **1** and **2**, *ortho* fluorines of o-BDC-F_4 are bound to the K(I) ion, while the other fluorines participate in the linkage of adjacent coordination layers forming 3-D supramolecular architectures via intermolecular F…F interactions. Spectroscopic, thermal, and fluorescence properties have been investigated. Variable-temperature magnetic susceptibility studies indicate that **1** displays a weak antiferromagnetic effect between adjacent Co(II) ions.

Keywords: Heterometallic-organic framework; Perfluorinated phthalate ligand; Crystal structure; Layered inorganic connectivity; Magnetic property

1. Introduction

Research on the discovery and synthesis of coordination polymers (CPs) or metal-organic frameworks (MOFs) remains an active and important area in crystal engineering, as well as

*Corresponding authors. Email: csc@cczu.edu.cn (S.-C. Chen); hmy@cczu.edu.cn (M.-Y. He)

coordination and materials chemistry, owing to interesting network structures and potential applications in gas storage, separation, luminescence, catalysis, and magnetism [1]. To realize the full potential, it is necessary to construct such crystalline materials with specific structures and functionality by deliberate design with appropriate selection of organic linkers and metal-containing units. Although fluorine-containing molecules are of particular interest as the strong electron-withdrawing effect of fluorine contributes to extraordinary functional properties and numerous applications [2], fluorinated organic ligands have scarcely been explored in inorganic–organic hybrids, especially MOFs or CPs. In this regard, MOFs with fluorinated *N*-containing heterocycle ligands (such as pyridine-type [3] and triazole-type compounds [4]) demonstrated remarkable abilities for induced-fit enclathration of organic molecules and high hydrogen adsorption. Perfluorinated aromatic dicarboxylic acids, such as tetrafluoroterephthalic acid (*p*-H_2BDC-F_4) [5], tetrafluoroisophthalic acid (*m*-H_2BDC-F_4) [6], tetrafluorophthalic acid (*o*-H_2BDC-F_4) [7], and 4,4′-(hexafluoroisopropylidene) bis(benzoic acid) (H_2hfbba) [8], have emerged as linkers for building fluorine-functionalized MOF materials since they have shown distinctive linking modes and peculiar variations in their physical properties when compared to their nonfluorinated analogs.

We are currently engaged in synthesis and coordination chemistry studies of perfluorinated dicarboxylic acid ligands under variable reaction conditions [7, 9]. In our previous work, a solvent-tuning strategy utilizing *o*-H_2BDC-F_4 was employed to construct two Cd (II) CPs [9(b)]. Very recently, we reported a convenient template-controlled method to prepare a series of isomeric water-soluble Ag(I) complexes with *o*-BDC-F_4, which show different 2-D-layered inorganic connectivities in solid state and exceptional antibacterial activity in aqueous solution [7(a)]. Previously, we demonstrated the alkali metal-templated assembly of Cd(II) CPs with *p*-BDC-F_4 [7(b)]. Mondal *et al.* reported a Dy^{III}-based MOF $\{[Dy(pyda)_3Ca_{1.5}(H_2O)_6]\cdot 5\cdot 5H_2O]\}$ (H_2pyda = pyridine-2,6-dicarboxylic acid) using Ca^{II} ions as structure-directing agents [10]. As a continuation of our work, we present two perfluorinated 2-D heterometallic-organic frameworks $[CoK_2(o\text{-BDC-}F_4)_2(MeOH)]_n$ (**1**) and $[MnK_2(o\text{-BDC-}F_4)_2(DMF)]_n$ (**2**) assembled from $M(OAc)_2$ (M = Co, Mn) and *o*-H_2BDC-F_4 in the presence of KNO_3. Both complexes have been characterized by single-crystal X-ray diffraction analyses, infrared (IR) spectra, elemental analyses, X-ray powder diffraction (XRPD), and thermogravimetric analyses (TGA). Fluorescence properties of **1** and **2** as well as the magnetic susceptibility of **1** have also been discussed.

2. Experimental

2.1. *Materials and general methods*

All chemicals were commercially available and used as received. Elemental analyses (C, H and N) were carried out on a PE-2400II (Perkin–Elmer) analyzer. IR spectra were recorded on a Nicolet ESP 460 FT-IR spectrometer with KBr pellets from 4000 to 400 cm^{-1}. TGA were performed on a Dupont thermal analyzer from room temperature to 800 °C (heating rate of 10 °C min^{-1}, nitrogen stream). The XRPD patterns were recorded on a Rigaku D/Max-2500 diffractometer at 40 kV and 100 mA for a Cu-target tube ($\lambda = 1.5406$ Å) and a graphite monochromator. Simulation of the XPRD spectra was carried out by single-crystal data and diffraction-crystal module of the Mercury program available free of charge via the Internet at http://www.iucr.org.

Magnetic data of **1** were collected using crushed crystals of the sample on a Quantum Design MPMS-XL SQUID magnetometer equipped with a 5 T magnet. The data were corrected using Pascal's constants to calculate the diamagnetic susceptibility, and an experimental correction for the sample holder was applied.

2.2. *Syntheses of complexes*

2.2.1. Synthesis of $[CoK_2(o\text{-}BDC\text{-}F_4)_2(MeOH)]_n$ (1). Complex **1** was prepared by mixing equal molar *o*-H_2BDC-F_4 (71.4 mg, 0.3 mmol), $Co(OAc)_2{\cdot}4H_2O$ (74.7 mg, 0.3 mmol), and KNO_3 (30.3 mg, 0.3 mmol) in MeOH/DMF mixed solvents (v/v, 9/3 mL). After *ca.* 30 min of stirring, the purple solution was filtered and left to stand at room temperature. After seven weeks, purple block crystals of **1** suitable for single-crystal X-ray diffraction were obtained by slow evaporation of the solvents in *ca.* 40% yield (77.3 mg, on the basis of *o*-H_2BDC-F_4). Anal. Calcd for $C_{17}H_7CoF_8K_2O_9$ (%): C, 31.69; H, 1.09. Found: C, 31.57; H, 1.08. IR (KBr, cm^{-1}): 3159 br, 2975 m, 2936 m, 1664 s, 1600 s, 1512 m, 1469 m, 1407 s, 1387 s, 1343 m, 1276 w, 1121 m, 1069 s, 953 s, 926 m, 867 m, 842 m, 815 w, 741 s, 708 m, 669 m, 616 w, 539 w, 496 w.

2.2.2. Synthesis of $[MnK_2(o\text{-}BDC\text{-}F_4)_2(DMF)]_n$ (2). The procedure was the same as that for **1** except that $Co(OAc)_2{\cdot}4H_2O$ was replaced with $Mn(OAc)_2{\cdot}4H_2O$ (73.5 mg, 0.3 mmol), affording yellow block crystals of **2** in *ca.* 55% yield (111.9 mg, on the basis of 1,2-H_2BDC-F_4). Anal. Calcd for $C_{19}H_7F_8K_2MnNO_9$ (%): C, 33.64; H, 1.04; N, 2.06. Found: C, 34.11; H, 1.03; N, 2.07. IR (KBr, cm^{-1}): 3540 m, 2958 m, 2923 m, 2823 m, 1631 s, 1591 s, 1513 m, 1469 s, 1426 s, 1384 s, 1343 m, 1275 m, 1130 m, 1071 s, 1017 m, 952 m, 848 m, 808 w, 772 s, 764 s, 728 m, 695 w, 616 w, 536 w, 498 w.

2.3. *X-ray crystallography*

Single-crystal X-ray diffraction measurements of **1** and **2** were performed on a Bruker Apex II CCD diffractometer at ambient temperature with Mo Kα radiation (λ = 0.71073 Å). A semi-empirical absorption correction was applied using *SADABS*, and the program *SAINT* was used for integration of the diffraction profiles [11]. The structures were solved by direct methods using *SHELXS* program of *SHELXTL* packages and refined anisotropically for all non-H atoms by full-matrix least squares on F^2 with *SHELXL* [12]. In general, hydrogens were located geometrically and allowed to ride during the subsequent refinement. O-bound hydrogens were first located in difference Fourier maps and then fixed geometrically with isotropic temperature factors. Further crystallographic data and structural refinement parameters are summarized in table 1; selected bond lengths and angles are listed in table 2.

3. Results and discussion

3.1. *Synthesis and general characterization*

Complexes **1** and **2** were prepared in the presence of KNO_3 with metal acetate at room temperature. When using other alkali metal salts such as LiOAc and NaOAc as potential

Table 1. Crystallographic data and structure refinement for **1** and **2**.

	1	**2**
Empirical formula	$C_{17}H_7F_8K_2CoO_9$	$C_{19}H_7F_8K_2MnNO_9$
Formula weight	644.36	678.40
Crystal size (mm^3)	$0.24 \times 0.22 \times 0.22$	$0.20 \times 0.20 \times 0.18$
Crystal system	Monoclinic	Monoclinic
Space group	*P2/c*	$P2_1/c$
a (Å)	7.132(1)	7.187(1)
b (Å)	13.664(2)	30.265(5)
c (Å)	11.167(1)	11.324(1)
α (°)	90	90
β (°)	112.426(8)	110.867(8)
γ (°)	90	90
V ($Å^3$)	1005.9(2)	2301.6(6)
Z	2	4
ρ_{Calcd} (g cm^{-3})	2.127	1.958
μ (cm^{-1})	1.395	1.054
F(0 0 0)	636	1340
Range of *h*, *k*, *l*	−8/7, −16/12, −13/13	−8/8, −35/31, −13/13
Total/independent reflections	5334/1777	12,371/4057
R_{int}	0.0436	0.0703
R^a, $R_w{}^b$	0.0472, 0.1263	0.0616, 0.1577
GOF[c]	1.070	1.098
Residuals (e $Å^{-3}$)	1.420, −0.779	0.875, −0.791

[a] $R = \sum ||F_o| - |F_c|| \; / \; \sum |F_o|$.

[b] $R_w = [\sum[w(F_o^2 - F_c^2)^2] \; / \; \sum w(F_o^2)^2]^{1/2}$.

[c] $\text{GOF} = \left\{\sum[w(F_o^2 - F_c^2)^2] \; / \; (n-p)\right\}^{1/2}$.

structure-directing agents, we were unable to isolate, under the same conditions, solid products suitable for X-ray analysis. Complexes **1** and **2** are stable under ambient conditions and consistent with the polymeric nature and are insoluble in water and common organic solvents. IR spectra of **1** and **2** show the antisymmetric and symmetric stretching vibrations of carboxylate in the range of 1590–1665 cm^{-1} and 1380–1470 cm^{-1}, respectively. Additionally, the absence of strong absorptions around 1740 and 1715 cm^{-1} for free *o*-H_2BDC-F_4 is characteristic of complete deprotonation of carboxyl groups in **1** and **2**. This is also confirmed by the X-ray structure analyses for **1** and **2**.

3.2. *Description of crystal structures*

X-ray diffraction studies of **1** and **2** reveal that they exhibit similar 2-D heterometallic-organic frameworks despite their different space groups and solvent ligands. Therefore, only the crystal structure of **1** will be described in detail. The asymmetric unit is made up of a half Co(II) ion, one K(I) ion, one *o*-BDC-F_4 dianion, and one methanol. As shown in figure 1(a), each Co(II) is six-coordinate octahedral provided by six oxygens from four *o*-BDC-F_4 ligands with Co–O bond distances 2.063(2)–2.228(2) Å. The K(I) is surrounded by seven oxygens from five *o*-BDC-F_4 ligands and one oxygen from methanol as well as one fluorine from one *o*-BDC-F_4 ligand [see figure 1(b)]. The K–O distances are 2.696–3.102(3) Å, and the K–F distance of 3.026 Å is similar to that of 3.009 Å observed in $[K_2(L)_2(tmeda)_2]$ (HL = *N*,*N*-diethyl-*N*′-2,3,5,6-tetrafluorophenylethane-1,2-diamine and tmeda = N,N,N′,N′-tetramethyl-1,2-ethanediamine) [13]. In **1**, *o*-BDC-F_4 takes an unusual μ_7-bridging mode

Table 2. Selected bond lengths (Å) and angles (°) for **1** and **2**[a].

*Complex **1***			
Co(1)–O(1)	2.145(2)	Co(1)–O(2)	2.228(2)
Co(1)–O(3)#2	2.036(2)	K(1)–O(1)#4	2.759(2)
K(1)–O(2)#5	2.859(2)	K(1)–O(2)#6	2.892(3)
K(1)–O(3)#4	3.031(3)	K(1)–O(3)#6	3.102(3)
K(1)–O(4)	2.696(3)	K(1)–O(4)#7	2.876(3)
K(1)–O(5)	2.780(3)	K(1)–F(1)	3.026(3)
O(1)–Co(1)–O(1)#1	91.1(1)	O(1)–Co(1)–O(2)	60.0(1)
O(1)–Co(1)–O(3)#2	178.0(1)	O(1)–Co(1)–O(3)#3	90.1(1)
O(1)#1–Co(1)–O(2)	91.3(1)	O(2)–Co(1)–O(2)#1	140.1(1)
O(2)–Co(1)–O(3)#2	118.4(1)	O(2)–Co(1)–O(3)#3	90.7(1)
O(3)#2–Co(1)–O(3)#3	88.7(1)	O(1)#4–K(1)–O(2)#5	139.9(1)
O(1)#4–K(1)–O(2)#6	116.7(1)	O(1)#4–K(1)–O(3)#4	68.6(1)
O(1)#4–K(1)–O(3)#6	60.8(7)	O(1)#4–K(1)–O(4)	127.0(8)
O(1)#4–K(1)–O(4)#7	130.3(1)	O(1)#4–K(1)–O(5)	64.5(1)
O(1)#4–K(1)–F(1)	83.6(1)	O(2)#5–K(1)–O(2)#6	103.5(1)
O(2)#5–K(1)–O(3)#4	138.4(1)	O(2)#5–K(1)–O(3)#6	146.4(1)
O(2)#5–K(1)–O(4)	70.0(1)	O(2)#5–K(1)–O(4)#7	63.9(1)
O(2)#5–K(1)–O(5)	77.1(1)	O(2)#5–K(1)–F(1)	77.7(1)
O(2)#6–K(1)–O(3)#4	62.1(1)	O(2)#6–K(1)–O(3)#6	64.3(1)
O(2)#6–K(1)–O(4)	65.7(1)	O(2)#6–K(1)–O(4)#7	67.1(1)
O(2)#6–K(1)–O(5)	162.3(1)	O(2)#6–K(1)–F(1)	119.3(1)
O(3)#4–K(1)–O(3)#6	66.1(1)	O(3)#4–K(1)–O(4)	68.5(1)
O(3)#4–K(1)–O(4)#7	128.0(1)	O(3)#4–K(1)–O(5)	128.9(1)
O(3)#4–K(1)–F(1)	77.5(1)	O(3)#6–K(1)–O(4)	123.6(1)
O(3)#6–K(1)–O(4)#7	82.8(1)	O(3)#6–K(1)–O(5)	105.3(1)
O(3)#6–K(1)–F(1)	135.8(1)	O(4)–K(1)–O(4)#7	100.6(1)
O(4)–K(1)–O(5)	129.2(1)	O(4)–K(1)–F(1)	57.9(1)
O(4)#7–K(1)–O(5)	98.2(1)	O(4)#7–K(1)–F(1)	141.1(1)
O(5)–K(1)–F(1)	78.3(1)		
*Complex **2***			
Mn(1)–O(1)	2.303(3)	Mn(1)–O(2)	2.254(3)
Mn(1)–O(3)#8	2.229(3)	Mn(1)–O(4)#8	2.603(3)
Mn(1)–O(5)	2.155(3)	Mn(1)–O(6)	2.541(3)
Mn(1)–O(8)#9	2.123(3)	K(1)–O(1)#8	2.902(3)
K(1)–O(3)#8	3.178(4)	K(1)–O(4)#12	2.749(4)
K(1)–O(5)	2.802(3)	K(1)–O(6)#11	2.811(3)
K(1)–O(7)#10	2.801(4)	K(1)–O(8)	3.268(4)
K(1)–O(9)	2.786(4)	K(1)–F(9)#12	2.897(3)
K(2)–O(1)	2.868(3)	K(2)–O(2)#11	2.841(4)
K(2)–O(3)#11	2.949(4)	K(2)–O(4)#8	3.051(4)
K(2)–O(6)#10	2.936(3)	K(2)–O(7)#13	2.808(4)
K(2)–O(8)#10	2.958(4)	K(2)–O(9)	2.711(4)
K(2)–F(8)#13	2.859(3)		
O(1)–Mn(1)–O(2)	57.6(1)	O(1)–Mn(1)–O(3)#8	125.3(1)
O(1)–Mn(1)–O(4)#8	72.5(1)	O(1)–Mn(1)–O(5)	101.7(1)
O(1)–Mn(1)–O(6)	145.0(1)	O(1)–Mn(1)–O(8)#9	94.1(1)
O(2)–Mn(1)–O(3)#8	175.5(1)	O(2)–Mn(1)–O(4)#8	128.7()
O(2)–Mn(1)–O(5)	94.3(1)	O(2)–Mn(1)–O(6)	95.2(1)
O(2)–Mn(1)–O(8)#9	90.0(1)	O(3)#8–Mn(1)–O(4)#8	53.4(4)
O(3)#8–Mn(1)–O(5)	88.5(1)	O(3)#8–Mn(1)–O(6)	83.4(1)
O(3)#8–Mn(1)–O(8)#9	86.4(1)	O(4)#8–Mn(1)–O(5)	107.3(1)
O(4)#8–Mn(1)–O(6)	135.4(1)	O(4)#8–Mn(1)–O(8)#9	82.0(1)
O(5)–Mn(1)–O(6)	55.1(1)	O(5)–Mn(1)–O(8)#9	163.5(1)
O(6)–Mn(1)–O(8)#9	108.6(1)	O(1)#8–K(1)–O(3)#8	62.6(1)
O(1)#8–K(1)–O(4)#12	62.0(1)	O(1)#8–K(1)–O(5)	115.4(1)
O(1)#8–K(1)–O(6)#11	103.0(1)	O(1)#8–K(1)–O(7)#10	67.1(1)
O(1)#8–K(1)–O(8)	63.1(1)	O(1)#8–K(1)–O(9)	159.5(1)

(*Continued*)

Table 2. (*Continued*).

Complex ***2***			
O(1)#8–K(1)–F(9)#12	119.5(1)	O(3)#8–K(1)–O(4)#12	113.8(1)
O(3)#8–K(1)–O(5)	61.2(9)	O(3)#8–K(1)–O(6)#11	150.9(1)
O(3)#8–K(1)–O(7)#10	84.3(1)	O(3)#8–K(1)–O(8)	62.6(1)
O(3)#8–K(1)–O(9)	106.5(1)	O(3)#8–K(1)–F(9)#12	133.7(1)
O(4)#12–K(1)–O(5)	118.4(1)	O(4)#12–K(1)–O(6)#11	74.9(1)
O(4)#12–K(1)–O(7)#10	104.5(1)	O(4)#12–K(1)–O(8)	61.8(1)
O(4)#12–K(1)–O(9)	136.3(1)	O(4)#12–K(1)–F(9)#12	59.4(1)
O(5)–K(1)–O(6)#11	141.3(1)	O(5)–K(1)–O(7)#10	132.5(1)
O(5)–K(1)–O(8)	64.6(1)	O(5)–K(1)–O(9)	67.6(1)
O(5)–K(1)–F(9)#12	81.6(1)	O(6)#11–K(1)–O(7)#10	66.7(1)
O(6)#11–K(1)–O(8)	136.2(1)	O(6)#11–K(1)–O(9)	78.3(1)
O(6)#11–K(1)–F(9)#12	75.1(1)	O(7)#10–K(1)–O(8)	128.7(1)
O(7)#10–K(1)–O(9)	95.5(1)	O(7)#10–K(1)–F(9)#12	141.5(1)
O(8)–K(1)–O(9)	129.6(1)	O(8)–K(1)–F(9)#12	77.5(1)
O(9)–K(1)–F(9)#12	80.8(1)	O(1)–K(2)–O(2)#11	140.6(1)
O(1)–K(2)–O(3)#11	135.5(1)	O(1)–K(2)–O(4)#8	58.8(1)
O(1)–K(2)–O(6)#10	100.7(1)	O(1)–K(2)–O(7)#13	67.5(1)
O(1)–K(2)–O(8)#10	145.5(1)	O(1)–K(2)–O(9)	75.8(1)
O(1)–K(2)–F(8)#13	78.4(1)	O(2)#11–K(2)–O(3)#11	66.3(1)
O(2)#11–K(2)–O(4)#8	137.1(1)	O(2)#11–K(2)–O(6)#10	118.6(1)
O(2)#11–K(2)–O(7)#13	125.1(1)	O(2)#11–K(2)–O(8)#10	64.5(1)
O(2)#11–K(2)–O(9)	69.4(1)	O(2)#11–K(2)–F(8)#13	79.6(1)
O(3)#11–K(2)–O(4)#8	133.9(1)	O(3)#11–K(2)–O(6)#10	65.5(1)
O(3)#11–K(2)–O(7)#13	68.5(1)	O(3)#11–K(2)–O(8)#10	69.1(1)
O(3)#11–K(2)–O(9)	132.9(1)	O(3)#11–K(2)–F(8)#13	74.0(1)
O(4)#8–K(2)–O(6)#10	68.7(1)	O(4)#8–K(2)–O(7)#13	97.0(1)
O(4)#8–K(2)–O(8)#10	86.7(1)	O(4)#8–K(2)–O(9)	90.4(1)
O(4)#8–K(2)–F(8)#13	136.9(1)	O(6)#10–K(2)–O(7)#13	64.9(1)
O(6)#10–K(2)–O(8)#10	64.3(1)	O(6)#10–K(2)–O(9)	156.4(1)
O(6)#10–K(2)–F(8)#13	119.4(1)	O(7)#13–K(2)–O(8)#10	123.4(1)
O(7)#13–K(2)–O(9)	131.2(1)	O(7)#13–K(2)–F(8)#13	59.2(1)
O(8)#10–K(2)–O(9)	105.2(1)	O(8)#10–K(2)–F(8)#13	136.2(1)
O(9)–K(2)–F(8)#13	83.2(1)		

[a]Symmetry transformations used to generate equivalent atoms. For 1, #1: $-x$, y, $-z-1/2$; #2: x, $-y$, $z-1/2$; #3: $-x$, $-y$, $-z$; #4: $-x$, y, $-z+1/2$; #5: $-x+1$, y, $-z+1/2$; #6: x, $-y$, $z+1/2$; #7: $-x+1$, $-y$, $-z+1$; For 2, #8: x, $-y+1/2$, $z-1/2$; #9: x, $-y+1/2$, $z+1/2$; #10: $x+1$, $-y+1/2$, $z+1/2$; #11: $1+x$, y, z; #12: x, y, $z-1$; #13: $x+1$, y, $z+1$.

to connect two Co(II) ions and five K(I) ions, where one carboxylate adopting a μ_4-$\eta^2:\eta^3$-bridging coordination mode links one Co(II) ion and three K(I) ions while the other one taking a μ_5-$\eta^2:\eta^3$-bridging mode bridges one Co(II) ion and four K(I) ions. The adjacent KO_8F polyhedra are linked to each other via O1 and O3 of carboxylate groups in an edge-sharing mode to form a tape along the [1 0 0] direction. Such 1-D motifs are connected by O5 of methanol through vertex-sharing to fulfill the 2-D inorganic layer, and meanwhile, the CoO_6 polyhedra are embedded [see figure 1(c)]. The tetrafluorine-substituted benzene rings project on both the sides of the layer. Such heterometallic-layered structures show extended inorganic connectivity in two directions, involving uncommon infinite K–O–Co linkages [14] along zero organic connectivity (I^2O^0) [15]. Further, such layers showing a parallel arrangement are connected by intermolecular F*cdots*F interactions (F2$\cdots$F4^{i} distance = 3.038 Å, i = x, $-y+1$, $z+1/2$; F3$\cdots$F3^{ii} distance = 2.957 Å, ii = $-x$, $-y+1$, $-z$) to generate a 3-D supramolecular network [see figure 1(d)], where the F$\cdots$F distances of 3.038 and 2.957 Å are comparable to the van der Waals radii of 2.94 Å [16].

3.3. *XRPD results*

In order to confirm the phase purity of the bulk materials, XRPD experiments were carried out for **1** and **2**. The experimental and computer-simulated patterns of **1** and **2** are shown in figure 2. Although the experimental patterns have a few un-indexed diffraction lines and some are slightly broadened in comparison with those simulated from single-crystal X-ray diffraction, the bulk synthesized materials and the crystalline material used for single-crystal X-ray studies were the same for both complexes.

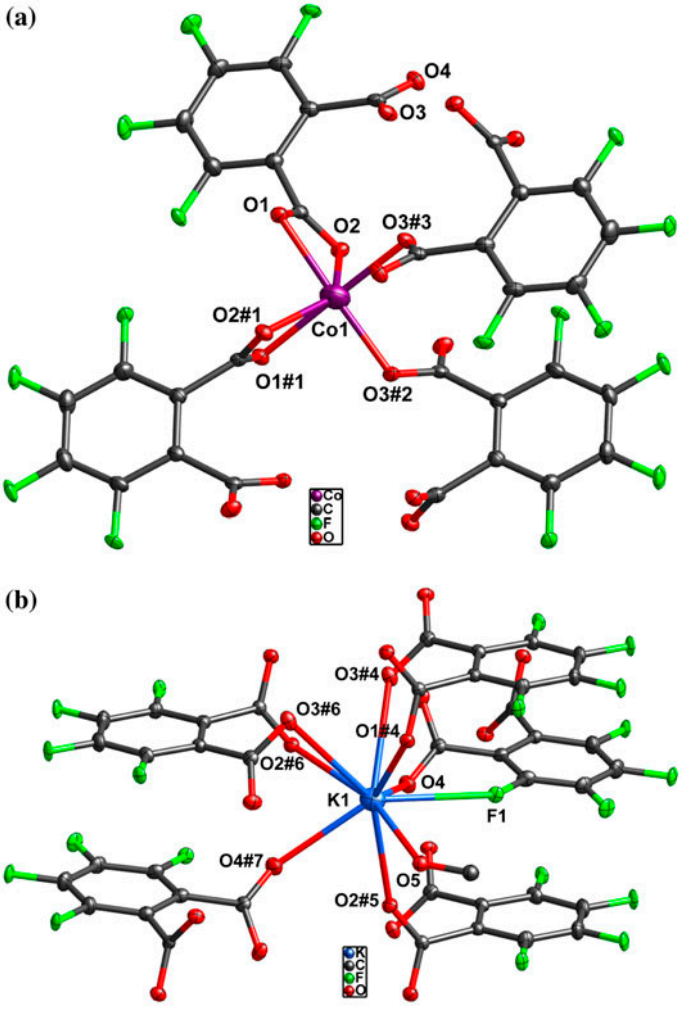

Figure 1. View of (a) the coordination environment of the Co(II) ion in **1** (symmetry codes: #1, $-x$, y, $-z-1/2$; #2, x, $-y$, $z-1/2$; #3, $-x$, $-y$, $-z$), (b) the coordination environment of the K(I) ion in **1** (symmetry codes: #4, $-x$, y, $-z+1/2$; #5, $-x+1$, y, $-z+1/2$; #6, x, $-y$, $z+1/2$; #7, $-x+1$, $-y$, $-z+1$), (c) the polyhedral representation of the 2-D K–O–Co inorganic connectivity of **1** with $Co(II)^{II}$ and K(I) ions highlighted in turquoise and pink polyhedra, respectively, and (d) the 3-D supramolecular framework of **1** through interlayer F⋯⋯F interactions (green dashed lines), and irrelevant hydrogens are omitted for clarity (see http://dx.doi.org/10.1080/00958972.2015.1057709 for color version).

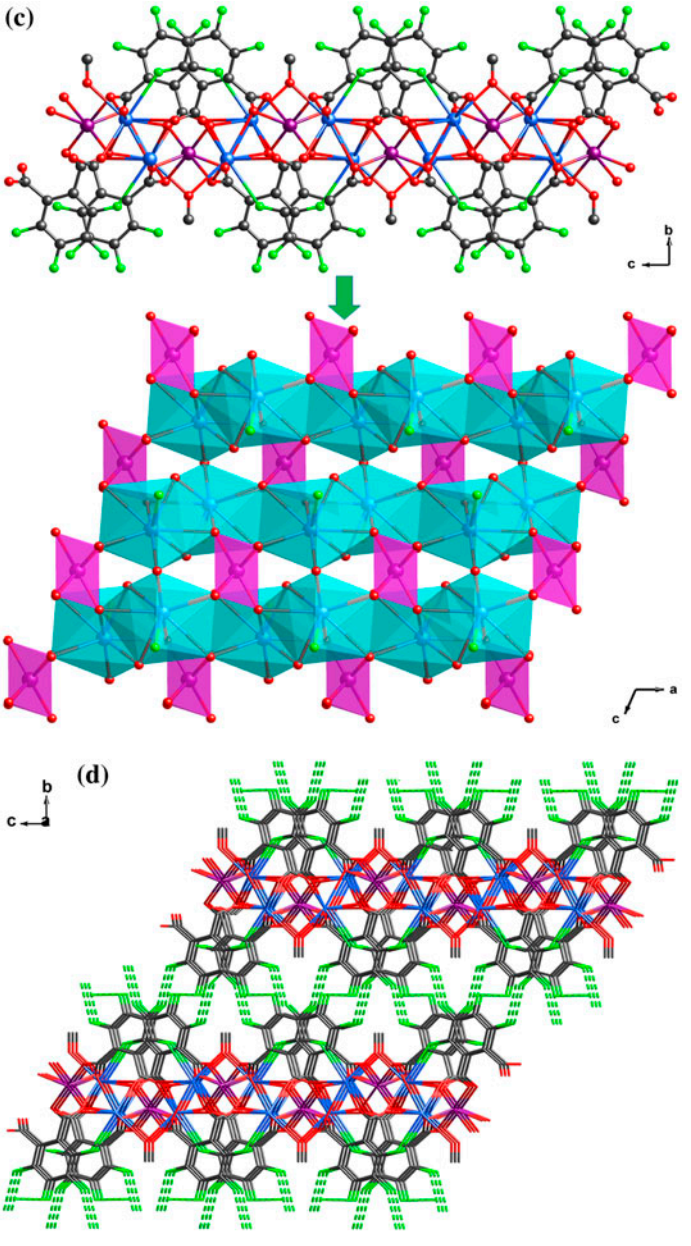

Figure 1. (*Continued*).

3.4. *TGA analyses*

TGA of **1** and **2** were performed by heating the crystalline samples under an atmosphere of N_2 between ambient temperature and 800 °C, and the corresponding curves are depicted in figure 3. The TGA curves of **1** and **2** are similar, probably due to their structural similarity. Both complexes exhibit high thermal stability with the mass remaining largely unchanged

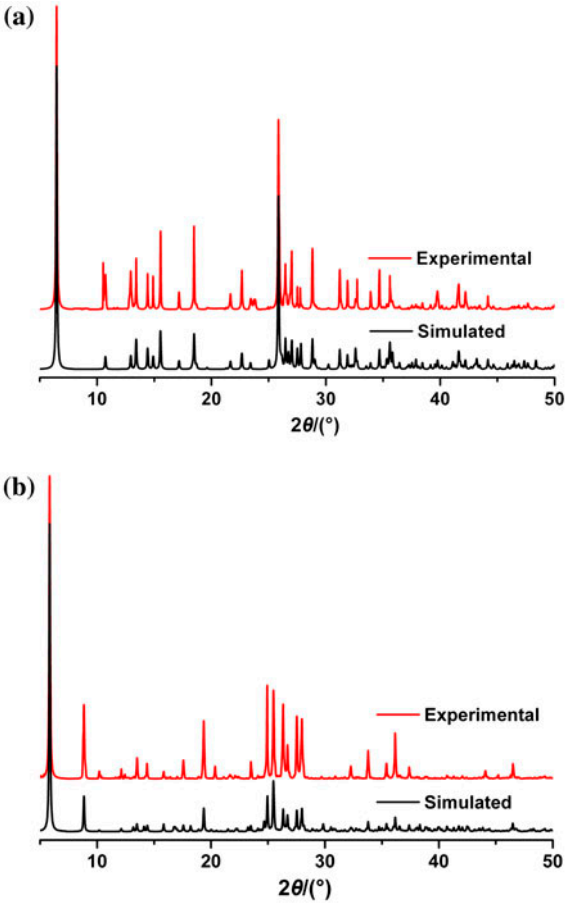

Figure 2. Experimental and simulated PXRD patterns for **1** (a) and **2** (b).

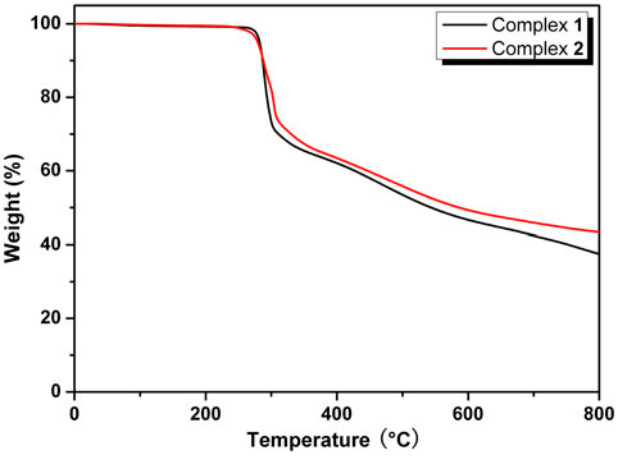

Figure 3. TGA curves of **1** and **2**.

until the decomposition onset temperature of approximately 260 °C. Critical weight losses at 260–330 °C indicate the pyrolysis of organic components. Further heating to 800 °C induces a further continuous and slow weight loss.

3.5. *Luminescent properties*

To explore potential applications as luminescent crystalline materials, the emission spectra of **1** and **2** as well as *o*-H_2BDC-F_4 were recorded in the solid state at room temperature (see figure 4). Excitation of the microcrystalline samples at 336 nm leads to generation of broad fluorescent emissions from 450 to 530 nm. Free *o*-H_2BDC-F_4 has a strong fluorescent emission band maximized at 478 nm, which can be ascribed to $\pi \rightarrow \pi^*$ and/or $n \rightarrow \pi^*$ transitions. In comparison with the spectrum of 1,2-H_2BDC-F_4, **1** and **2** show similar weak emissions maximized at 477 nm for **1** and 475 nm for **2**. The emission bands of both complexes likely originate from the ligand-centered transitions. Furthermore, the emission

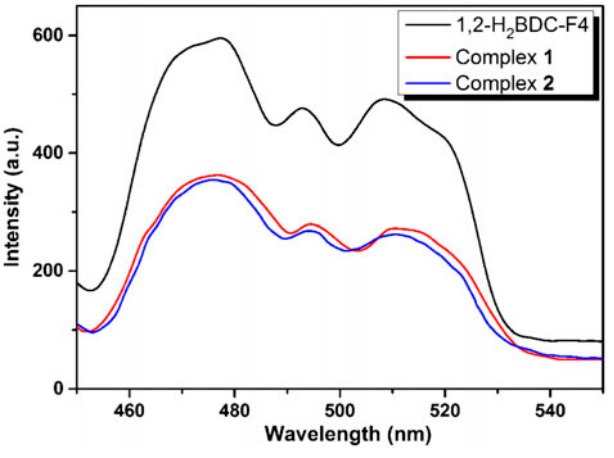

Figure 4. Solid-state fluorescent emission spectra of free *o*-H2BDC-F4, **1** and **2**.

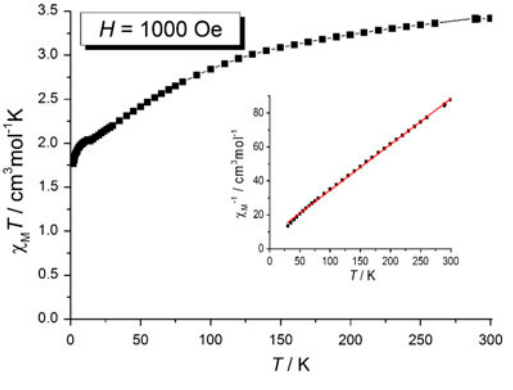

Figure 5. Temperature dependence of the $\chi_M T$ product at 1000 Oe for **1**. Inset: Plot of $\chi_M^{-1}\chi M^{-1}$ *vs.* *T* (solid red line represents a fit to the high temperature region above 30 K according to the Curie–Weiss law) (see http://dx.doi.org/10.1080/00958972.2015.1057709 for color version).

intensities of **1** and **2** are significantly weaker than that of the free ligand, which is likely related to complicated structures as well as the decay effect of high-energy C–H and/or O–H oscillators from the coordinated solvent [17].

3.6. *Magnetic studies*

Variable-temperature direct current (dc) magnetic susceptibility data of **1** were measured on polycrystalline samples from 2 to 300 K with an applied magnetic field of 1000 Oe as shown in figure 5. The $\chi_M T$ value at 300 K is 3.42 $cm^3\ mol^{-1}$ K, which is larger than the spin-only value (1.875 $cm^3\ mol^{-1}$ K, $S = 3/2$, $g = 2$) for the high-spin octahedral Co(II) ion as a consequence of unquenched orbital angular momentum [18]. Upon cooling, the $\chi_M T$ value decreases to 1.76 $cm^3\ mol^{-1}$ K at 2 K. Fitting of the data above 30 K to the Curie–Weiss law gives a negative Weiss constant $\theta = -28.12$ K and a Curie constant (C) of 3.71 $cm^3\ mol^{-1}$ K. The negative θ value and the decrease in $\chi_M T$ above 30 K suggest the antiferromagnetic interaction between the shortest Co(II)−Co(II) distance.

4. Conclusion

We report two 2-D K(I)-M(II) (M = Mn and Co) heterometallic-organic frameworks based on a perfluorinated phthalate ligand, giving K–O–M inorganic connectivities. Both complexes show strong K–F coordination, and an investigation on the crystal packing suggests that intermolecular F···F interactions may act as important driving forces for the assembly of these 3-D supramolecular architectures, which further enrich our knowledge of metal-fluorocarbon coordination chemistry and supramolecular fluorine chemistry. In addition, weak antiferromagnetic interaction exists between Co(II) ions.

Supplementary material

CCDC 1037711 and 1037712 contain the supplementary crystallographic data for **1** and **2**. These data can be obtained free of charge from the Cambridge Crystallographic Data Center via http://www.ccdc.cam.ac.uk/conts/retrieving.html (or from the CCDC, 12 Union Road, Cambridge CB2 1EZ, UK; Fax: +44 1223 3360 33; Email: deposit@ccdc.cam.ac.uk).

Disclosure statement

No potential conflict of interest was reported by the authors.

Funding

This work was supported by the National Natural Science Foundation of China [grant number 21201026]; the Nature Science Foundation of Jiangsu Province [grant number BK20131142]; a Project Funded by the Priority Academic Program Development of Jiangsu Higher Education Institutions (PAPD).

References

[1] (a) M.P. Suh, H.J. Park, T.K. Prasad, D.-W. Lim. *Chem. Rev.*, **112**, 782 (2012); (b) J.-R. Li, J. Sculley, H.-C. Zhou. *Chem. Rev.*, **112**, 869 (2012); (c) Y. Cui, Y. Yue, G. Qian, B. Chen. *Chem. Rev.*, **112**, 1126 (2012); (d)

M. O'Keeffe, O.M. Yaghi. *Chem. Rev.*, **112**, 675 (2012); (e) W. Zhang, R.-G. Xiong. *Chem. Rev.*, **112**, 1163 (2012); (f) N.W. Ockwig, O. Delgado-Friedrichs, M. O'Keeffe, O.M. Yaghi. *Acc. Chem. Res.*, **38**, 176 (2005); (g) H.-L. Gao, L. Yi, B. Zhao, X.-Q. Zhao, P. Cheng, D.-Z. Liao, S.-P. Yan. *Inorg. Chem.*, **45**, 5980 (2006).
[2] (a) C. Limban, M.C. Chifiriuc. *Int. J. Mol. Sci.*, **12**, 6432 (2011); (b) J.D. Dunitz. *Chem. Biochem.*, **5**, 614 (2004); (c) J.A. Gladysz, D.P. Curran, I.T. Horváth. *Handbook of Fluorine Chemistry*, Wiley/VCH, Weinheim (2004).
[3] K. Kasai, M. Aoyagi, M. Fujita. *J. Am. Chem. Soc.*, **122**, 2140 (2000).
[4] C. Yang, X. Wang, M.A. Omary. *J. Am. Chem. Soc.*, **129**, 15454 (2007).
[5] (a) B. Chen, Y. Yang, F. Zapata, G. Qian, Y. Luo, J. Zhang, E.B. Lobkovsky. *Inorg. Chem.*, **45**, 8882 (2006); (b) C. Seidel, R. Ahlers, U. Ruschewitz. *Cryst. Growth Des.*, **11**, 5053 (2011); (c) C. Seidel, C. Lorbeer, J. Cybinska, A.-V. Mudring, U. Ruschewitz. *Inorg. Chem.*, **51**, 4679 (2012).
[6] Z. Wang, V.C. Kravtsov, R.B. Walsh, M.J. Zaworotko. *Cryst. Growth Des.*, **7**, 1154 (2007).
[7] (a) S.-C. Chen, Z.-H. Zhang, Q. Chen, L.-Q. Wang, J. Xu, M.-Y. He, M. Du, X.-P. Yang, R.A. Jones. *Chem. Commun.*, **49**, 1270 (2013); (b) S.-C. Chen, Z.-H. Zhang, K.-L. Huang, H.-K. Luo, M.-Y. He, M. Du, Q. Chen. *Cryst. Eng. Commun.*, **15**, 9613 (2013); (c) S.-C. Chen, F. Tian, K.-L. Huang, C.-P. Li, J. Zhong, M.-Y. He, Z.-H. Zhang, H.-N. Wang, M. Du, Q. Chen. *Cryst. Eng. Commun.*, **16**, 7673 (2014).
[8] P. Pachfule, C. Dey, T. Panda, R. Banerjee. *Cryst. Eng. Commun.*, **12**, 1600 (2010).
[9] (a) S.-C. Chen, Z.-H. Zhang, Q. Chen, H.-B. Gao, Q. Liu, M.-Y. He, M. Du. *Inorg. Chem. Commun.*, **12**, 835 (2009); (b) S.-C. Chen, Z.-H. Zhang, M.-Y. He, H. Xu, Q. Chen. *Z. Anorg. Allg. Chem.*, **636**, 824 (2010).
[10] B. Mondal, B. Sen, E. Zangrando, P. Chattopadhyay. *J. Chem. Sci*., **126**, 1115 (2014).
[11] Bruker AXS. *SAINT Software Reference Manual*, Bruker AXS, Madison, WI (1998).
[12] G.M. Sheldrick. *SHELXTL NT Version 5.1, Program for Solution and Refinement of Crystal Structures*, University of Göttingen, Germany (1997).
[13] G.B. Deacon, C.M. Forsyth, P.C. Junk, J. Wang. *Chem. Eur. J.*, **15**, 3082 (2009).
[14] S. Xiang, Y. He, Z. Zhang, H. Wu, W. Zhou, R. Krishna, B. Chen. *Nat. Commun.*, **3**, 954 (2012).
[15] A.K. Cheetham, C.N.R. Rao, R.K. Feller. *Chem. Commun.*, **46**, 4780 (2006).
[16] L.J. Han, L.Y. Fan, M. Meng, X. Wang, C.Y. Liu. *Dalton Trans.*, **40**, 12832 (2011).
[17] B. Chen, Y. Yang, F. Zapata, G. Qian, Y. Luo, J. Zhang, E.B. Lobkovsky. *Inorg. Chem.*, **45**, 8882 (2006).
[18] (a) F.E. Mabbs, D.J. Machin. *Magnetism and Transition Metal Complexes*, Dover Publications Inc, Mineola (2008); (b) M. Kurmoo. *Chem. Soc. Rev.*, **38**, 1353 (2009).